BIOCHEMISTRY
including biophysical chemistry & molecular biology
Article

Biochemistry **2009,** *48,* 10089–10097 10089
DOI: 10.1021/bi900916t

Oligosaccharide Binding in *Escherichia coli* Glycogen Synthase[†,‡]

Fang Sheng,[§,¶] Alejandra Yep,[∥,⊥] Lei Feng,[§] Jack Preiss,[∥] and James H. Geiger*[,§]

[§]*Department of Chemistry and* [∥]*Department of Biochemistry and Molecular Biology, Michigan State University, East Lansing, Michigan 48824.* [⊥]*Current address: College of Pharmacy, University of Michigan, Ann Arbor, Michigan 48109.* [¶]*Current address: Department of Chemistry and Biochemistry, University of California Los Angeles, 611 Charles Young Dr. East, Los Angeles, California 90095-1569.*

Received June 1, 2009; Revised Manuscript Received September 15, 2009

ABSTRACT: Glycogen/starch synthase elongates glucan chains and is the key enzyme in the synthesis of glycogen in bacteria and starch in plants. Cocrystallization of *Escherichia coli* wild-type glycogen synthase (GS) with substrate ADPGlc and the glucan acceptor mimic HEPPSO produced a closed form of GS and suggests that domain−domain closure accompanies glycogen synthesis. Cocrystallization of the inactive GS mutant E377A with substrate ADPGlc and oligosaccharide results in the first oligosaccharide-bound glycogen synthase structure. Four bound oligosaccharides are observed, one in the interdomain cleft (G6a) and three on the N-terminal domain surface (G6b, G6c, and G6d). Extending from the center of the enzyme to the interdomain cleft opening, G6a mostly interacts with the highly conserved N-terminal domain residues lining the cleft of GS. The surface-bound oligosaccharides G6c and G6d have less interaction with enzyme and exhibit a more curled, helixlike structural arrangement. The observation that oligosaccharides bind only to the N-terminal domain of GS suggests that glycogen in vivo probably binds to only one side of the enzyme to ensure unencumbered interdomain movement, which is required for efficient, continuous glucan-chain synthesis.

Glycogen synthase (GS)[1] and starch synthase (SS) produce the long α-1,4-linked glucan chain that forms the backbone of glycogen in bacteria and starch in plants, using ADP-glucose (ADPGlc) as a sugar donor (*1*). They share 32−40% sequence identity, and both are members of the GT5 glycosyl transferase (GT) family whose members all share the GT-B fold (*2*, *3*). GT-B fold enzymes are comprised of two domains separated by an interdomain cleft where the active site is located.

Our structural studies of apo double mutant C7S/C409S (dmGS) and ligand-bound wild-type *Escherichia coli* GS (wtGS) as well as previously reported *Agrobacterium tumefaciens* GS (AtGS) and *Pyrococcus abyssi* GS (PaGS) structures suggest that a large interdomain motion is required to form the active site of GS (*4*−*6*). It appears from the structural evidence that this interdomain closure requires the binding of both ADPGlc and glucan, as structures that lack either ADP or ADPGlc but lack a glucan or glucan mimic adopt their open conformation (*4*, *5*). This model therefore postulates that interdomain motion accompanies glucan elongation catalyzed by GS. Specifically, the two domains approach each other and generate a competent active site for transfer of glucose from the substrate ADPGlc to the growing glucan acceptor. Once this step is completed, the two domains must then open to release the elongated glucan chain and the product ADP in anticipation of the next turnover. It is therefore critically important to understand the manner in which long-chain glucans bind GS both within and outside of the active site of the enzyme.

To date, there is no structure of an oligosaccharide bound at the active site for GS, SS, or glycogen phosphorylase (GP), though the first structure of GP was published in the 1970s (*7*, *8*). The maltopentaose (G5)- or maltoheptaose (G7)-incubated GP resulted in oligosaccharides binding in the glycogen storage site, and the glucans were in helical conformations (*9*) as previously suggested for glycogen (*10*, *11*). However, a structure of maltodextrin phosphorylase (MalP), another GT-B-retaining enzyme similar to glycogen phosphorylase, bound to G5 does show oligosaccharide binding in the active site (*12*, *13*). The G5 in the MalP complex reveals a kink between the +1 and −1 sugars. Although most of the active site residues are conserved in MalP, GS and SS, the residues responsible for glucan binding are significantly less so. Thus, it is less clear that glucans will bind similarly in the structures.

In contrast, the maltoporin−glucan structure shows long malto-oligosaccharides bound in a channel and retaining a helical conformation. On the basis of this evidence, translocation was proposed to proceed in a screwlike fashion (*14*). The smooth surface of a greasy slide made of continuous aromatic amino acid side chains punctuated by multiple hydrogen bonds may allow glucan translocation with a relatively low energy barrier. We noticed that there are several aromatic residues in the GS interdomain cleft, suggesting that a similar mechanism was possible for GS.

To elucidate the structural basis of glycogen binding to GS, we have determined structures of a catalytically inactive E377A mutant GS bound to maltohexaose. In this paper, we describe in detail the modes of binding of oligosaccharides to GS, both in the active site and on the surface of the N-terminal domain. Our

[†]This research was supported by Department of Energy Grant DE-FG02-06ER15822 from the Office of Energy Biosciences (to J.H.G.) and Research Grant IS-3733-05R from BARD (to J.P.).

[‡]Crystallographic coordinates have been deposited in the Protein Data Bank as entry 3CX4.

*To whom correspondence should be addressed. Telephone: (517) 355-9715, ext. 234. Fax: (517) 355-1793. E-mail: geiger@cem.msu.edu.

[1]Abbreviations: ADPGlc, ADP-glucose; HEPPSO, *N*-(2-hydroxyethyl)piperazine-*N*′-2-hydroxypropanesulfonic acid; AtGS, *Agrobacterium tumefaciens* GS; GBSS, granule-bound starch synthase; GP, glycogen phosphorylase; GS, glycogen synthase; GT, glycosyltransferase; G5, maltopentaose; G6, maltohexaose; SS, starch synthase; MalP, maltodextrin phosphorylase; PaGS, *Pyrococcus abyssi* GS; PDB, Protein Data Bank; PLP, pyridoxal phosphate; rmsd, root-mean-square deviation.

Published on Web 09/17/2009

results imply that the GS N-terminal domain contains the binding sites for long-chain glycans, with no evidence for cross-domain glycan interactions, consistent with the idea that substrates bind independently to the two domains with closure only occurring upon both substrates binding. These results are also discussed in terms of various starch synthase enzymes.

EXPERIMENTAL PROCEDURES

Protein Expression, Purification, and Crystallization. *E. coli* GS mutant E377A was overexpressed in *E. coli* and purified as described previously (*15*). The purified proteins were then buffer-exchanged into 20 mM triethanolamine HCl (pH 7.5) and 5 mM DTT before being concentrated to ~5−9 mg/mL.

E. coli GS E377A (8.6 mg/mL) was cocrystallized with 5 mM ADPGlc and 5 mM G6 in buffer consisting of 40% (w/v) PEG 4000 and 0.1 M 4-(2-hydroxyethyl)piperazine-*N*′-2-hydroxypropanesulfonic acid (HEPPSO) (pH 7.5). Crystals with dimensions of 0.05 mm × 0.05 mm × 0.05 mm were observed after 4 weeks, and to the 3 μL crystal-containing drop was added a 2 μL soaking solution containing well solution and 100 mM maltopentaose.

After 48 h, the G5-soaked crystal was harvested into a solution of the mother liquor with 15% glycerol as the cryoprotectant and flash-frozen. Diffraction data were collected at the Advanced Photon Source DND-CAT, BM-5 beamline (Argonne National Laboratory, Argonne, IL) to 2.29 Å resolution and reduced and scaled with X-GEN (*16*). One molecule was found per asymmetric unit. Other crystal parameters and detailed data collection statistics are listed in Table 1.

Structure Determination and Refinement. The structure was initially positioned using MOLREP (Collaborative Computational Project, CCP4) (*17*) using the *E. coli* GS wtGSb (PDB entry 2QZS) structure as a search model. Refinement and map calculations were conducted with REFMAC5 (CCP4) (*17*). All model building, including manual adjustments and fitting of carbohydrate density, was performed using TURBO-FRODO (*18*). Water molecules (201 total, with an average *B* factor of 56.7) were added using Coot and inspected visually prior to deposition. Five percent of the reflections were flagged as "free" (*19*) and used to monitor the refinement. The final model has good stereochemistry as evaluated by PROCHECK (CCP4) (see Table 1 for pertinent values) (*17*). The refined protein structure has high *B* factors (51 Å^2), but this value was consistent with the value suggested by the Wilson plot (62 Å^2).

Table 1: Data and Model Statistics of the *E. coli* GS E377A−ADP−G6 Complex

Data Processing Statistics	
resolution[a] (Å)	97.13−2.29 (2.35−2.29)
total no. of reflections[a]	335515 (25704)
multiplicity[a]	3.21 (2.47)
completeness[a] (%)	98.1 (99.0)
R_{merge}[a,b] (%)	8.5 (52.84)
I/σ[a,c]	14.5 (1.06)
Refinement Statistics	
R_{work}[d] (%)	18.60
R_{free}[e] (%)	22.10
rmsd	
bond lengths (Å)	0.011
bond angles (deg)	1.43
Ramachandran Statistics	
most favored (%)	90.4
additionally allowed (%)	9.3
generously allowed (%)	0.2
B Factor[f]	
average *B* (Å^2)	48.42
protein	49.32
ADP	47.35
waters (201 total)	56.7
oligosaccharide at the G6a site	53.48
oligosaccharide at the G6b site	92.80
oligosaccharide at the G6c site	68.98
oligosaccharide at the G6d site	65.50
Protein Data Bank entry	3CX4

[a]The values in parentheses are those for the outermost shell. [b]$R_{merge} = \sum_h\sum_i|I(h) - I_i(h)|/\sum_h\sum_i I_i(h)$, where $I_i(h)$ and $I(h)$ are the *i*th and mean measurements of the intensity of reflection *h*, respectively. [c]I/σ is the average ratio of the intensity and standard deviation of all reflections *h* after averaging over their occurrences *i*. [d]$R_{cryst} = \sum_h|F_o - F_c|/\sum_h F_o$, where F_o and F_c are the observed and calculated structure factor amplitudes of reflection *h*, respectively. [e]R_{free} is calculated as R_{cryst} with reflections that were excluded from the refinement (5% of the data). [f]G6a−d indicate the four oligosaccharide binding sites in the interdomain cleft, near the cleft opening, near loop 123−129, and loop 184−193, respectively.

RESULTS

Our previous results suggest that both ADPGlc and either a glucan or glucan mimic are required to produce the catalytically competent, closed conformation of GS. We have therefore used the catalytically inactive, E377A mutant to cocrystallize the mutant GS in the presence of both ADPGlc and maltohexaose. The previous structures of the E377A−ADPGlc−HEPPSO and wt ECGS−ADP−glucose−HEPPSO complexes together showed that E377 has dual roles in catalysis. It provides charge stabilization to Lys305, which in turn stabilizes the negative charge on the leaving group ADP, and it is critical in locating the acceptor glucose moiety.

The refined structure contains virtually the entire polypeptide chain lacking only the His-6 tag and the C-terminal Lys477. The overall enzyme structure is very similar to that of the E377A−ADP−HEPPSO structure, with the twin Rossmann fold domains rotated together and adopting the catalytically competent, closed conformation of the enzyme (Figure 1A) (*6*). The rmsd between the two structures is in fact only 0.44 Å. A summary of the X-ray data and refinement statistics for the *E. coli* E377A−ADP−G6 complex is shown in Table 1. The electron density clearly shows four GS-bound oligosaccharides (Figure 1B and Figures 1 and 2 of the Supporting Information). Oligosaccharide residues are numbered from the reducing end to the nonreducing end. They are numbered sequentially, beginning with G6a and ending with G6d, though it should be remembered that four distinct malto-oligosaccharides are bound to the enzyme.

The structure of *E. coli* GS E377A in complex with ADP and oligosaccharides exhibits a typical GT-B fold organization, with two Rossmann domains similar in size (N-terminus, residues 1−241; C-terminus, residues 250−457) and helical tail α18 (residues 458−476) returning from the C-terminal domain to the N-terminal domain (Figure 1A). No changes are seen to the helical tail between opened and closed conformations as there is an intervening linker sequence that connects the C-terminal tail to the rest of the C-terminus that serves as one of the hinge regions for the conformational change (*6*). The σ-weighted difference Fourier map ($2F_o - F_c$) of the E377A GS−ADP−G6 complex showed continuous density in the interdomain active site

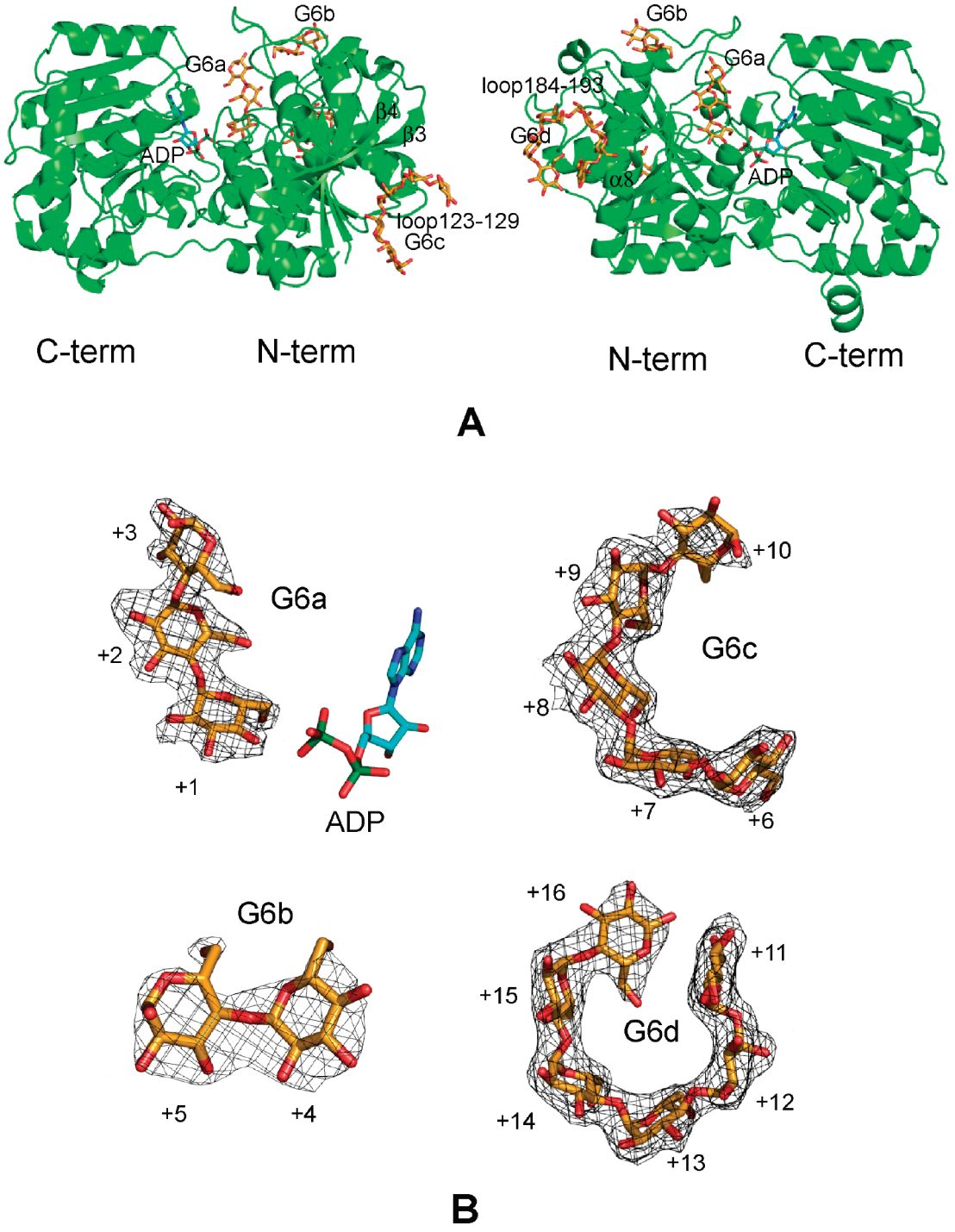

FIGURE 1: (A) Overall structure of *E. coli* GS E377A in complex with ADP and oligosaccharides. ADP and oligosaccharides are shown as sticks (ADP carbons, cyan; oligosaccharide carbons, orange; oxygens, red; phosphates, green). The secondary structure elements that host residues interacting with surface-bound oligosaccharides G6c and G6d are labeled. (B) $2F_o - F_c$ electron density map contoured at 1σ with built-in maltotriose at the G6a site, maltose at the G6b site, maltopentaose at the G6c site, and maltohexaose at the G6d site. The ADP molecule is shown for reference. All atoms colored as in panel A.

cleft ("G6a site"), corresponding to three well-defined glucose moieties extending from the active site toward the enzyme surface. All protein residues that directly contact this oligosaccharide are well-defined in the electron density map, and the interaction scheme is illustrated in Figure 2. No density is evident in the −1 site, however, where the ADP-glucose donor would be. This is consistent with our structure of the E377A EcGS mutant crystallized in the presence of ADPGlc and HEPPSO, which also showed no evidence of a glucose moiety at the −1 position (*6*). This was in contrast to the wild-type EcGS also crystallized in the presence of ADPGlc and HEPPSO, which showed well-defined density for a glucose molecule at this site. The difference is rationalized as being due to the loss of the critical interaction between the side chain of Glu377 and O3 of the glucose moiety in the E377A mutant, resulting in the loss of the enzyme's ability to bind a glucose moiety at the −1 position.

The +1 sugar is buried close to the ADP in the interdomain cleft (Figure 1A). Its 4-hydroxyl makes a hydrogen bond (2.6 Å) to the ADP phosphate O3B atom (Figure 2). Bidentate hydrogen bonds are made between the 2- and 3-hydroxyls and the Asp137

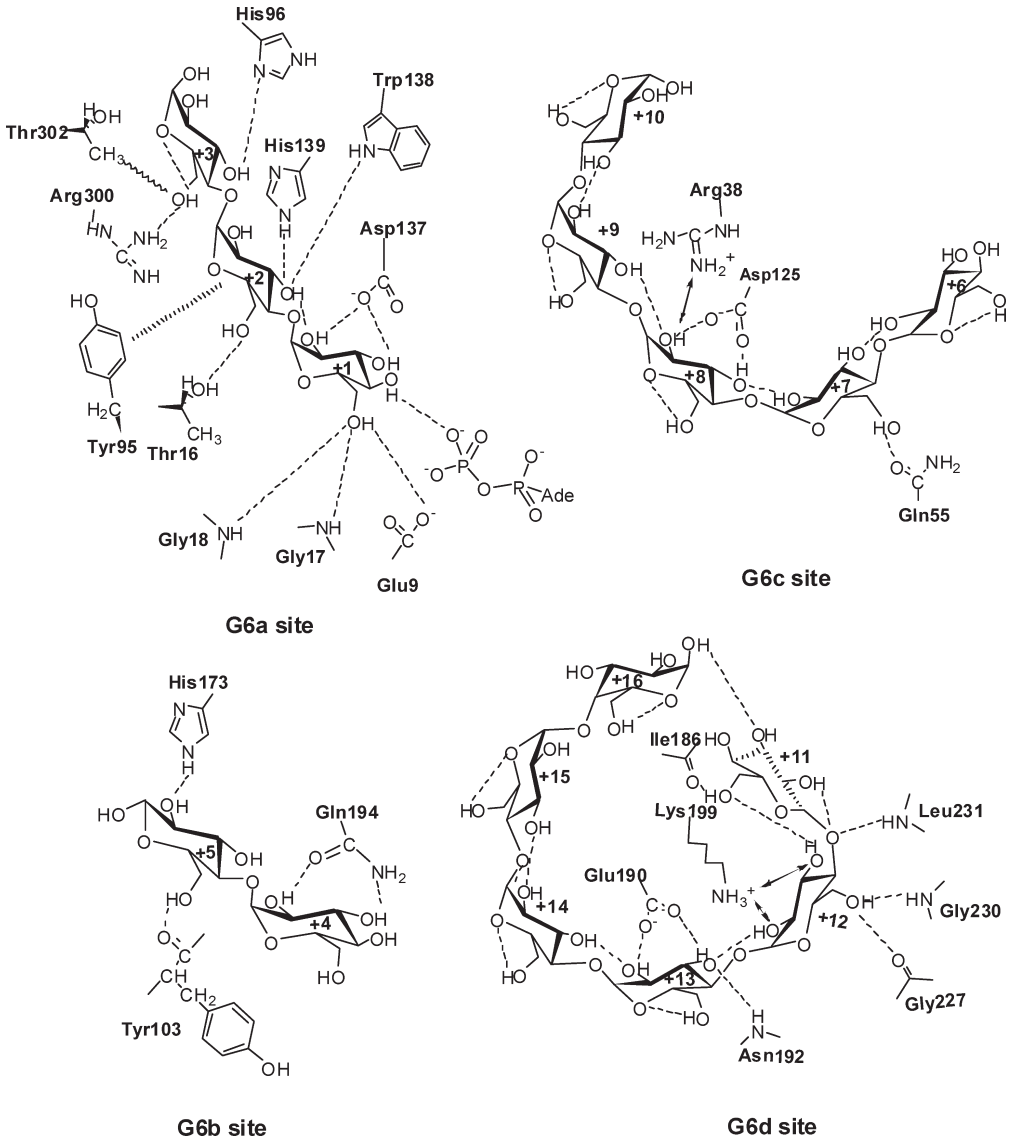

FIGURE 2: Schematic diagram of interactions between bound oligosaccharides and enzyme GS.

OD2 atom (2.4 and 2.7 Å, respectively). Its 6-hydroxyl group is close to the loop (containing residues 9−19) that hosts the K_{15}TGGL motif, which is highly conserved throughout the GS and SS family (Figure 3). The 6-hydroxyl of the +1 sugar makes hydrogen bonds with the backbone amides of Gly17 (2.9 Å) and Gly18 (3.1 Å), and with the side chain of Glu 9 (3.3 Å) (Figure 2).

The sugar at subsite +2 stacks against Tyr95 (3.80 Å), forming the lone aromatic stacking interaction between the bound oligosaccharide and GS (Figure 2). The 3-hydroxyl makes interactions with the His139 imidazole NE2 atom (2.8 Å) and Trp138 indole NE1 atom (2.9 Å). The 6-hydroxyl makes a hydrogen bond to the Thr16 side chain (3.2 Å). The sugar at subsite +3 interacts with the His96 ND1 atom via its 3-hydroxyl (2.85 Å). In addition, its 6-hydroxyl group makes a hydrogen bond to the Arg300 amide and is in van der Waals contact with Thr302, which represent the only interactions between any oligosaccharide and the GS C-terminal domain.

Three other oligosaccharide chains are observed at G6b, G6c, and G6d sites on the N-terminal domain surface (Figure 1A). The G6b site is close to the interdomain cleft opening, and the +4 sugar at the G6b site is approximately 6.5 Å from the +3 sugar at the G6a site. In contrast, the G6c and G6d sites are quite far from the interdomain cleft opening, and the shortest distances between the G6a and G6c oligosaccharides and between the G6a and G6d oligosaccharides are approximately 29 and 22 Å, respectively. Two glucose rings (+4 and +5) are found at the G6b site, and the electron density map is shown in Figure 1B. The +4 sugar OH-2 and OH-3 groups interact with the Gln194 side chain (2.73 and 3.09 Å, respectively). The +5 sugar 2-hydroxyl forms a close hydrogen bond to the His173 Ne atom (2.39 Å). The +5 sugar 6-hydroxymethyl group is within hydrogen bonding distance of the Tyr103 main-chain oxygen (3.22 Å) (Figure 1B).

The oligosaccharide at the G6c site consists of five glucose rings and is near the β3 (residues 55−58) and β4 (69−73) strands of the β-sheet, and the loop encompassing residues 123−129 (Figure 1). The oligosaccharide at G6d is comprised of six glucose units and is located between helix α8 (residues 229−237) and the loop containing residues 184−193 (connecting α5 and β9) (Figure 1A). Unlike the extended oligosaccharide residing in the G6a interdomain channel-binding site, both G6c and G6d adopt an almost circular conformation reminiscent of a cyclodextrin (Figure 2).

The oligosaccharide at the G6c site interacts with GS only at subsites +7 and +8 (Figure 2). The +7 sugar's 6-hydroxyl group

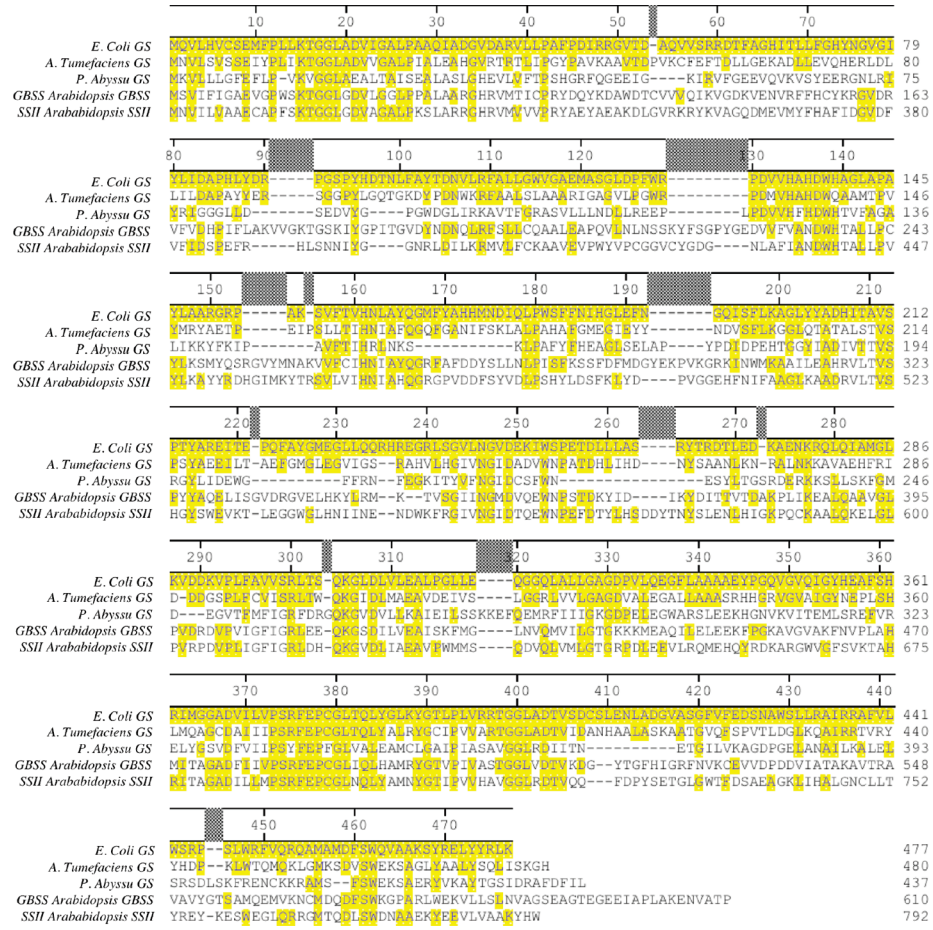

FIGURE 3: Sequence alignment of glycogen synthase and starch synthase enzymes. The organism for each is given. The GenBank accession numbers are P08323 (*E. coli*) (*20*), NP_534560 (*A. tumefaciens*) (*21*, *22*), NM_103023 (*Arabidopsis thaliana* GBSS), and NM_110984 (*A. thaliana* SS II). Residues that are identical to *E. coli GS* are shaded yellow. Alignment was performed using the DNASTAR program suite.

makes a hydrogen bond with the Gln55 NE2 atom (3.16 Å). The Asp125 carboxyl group forms tight, "double-handle" hydrogen bonds with the 2- and 3-hydroxyl groups of the +8 sugar (with distances of 2.5 and 2.60 Å, respectively). In addition, the +8 sugar 2-hydroxyl contacts the Arg38 side chain (2.97 Å).

The oligosaccharide at G6d is the most circular oligosaccharide among the four bound to GS. In fact, the initial (+11) sugar's 3-hydroxyl makes a 2.65 Å hydrogen bond with the +16 sugar's 1-hydroxyl, stabilizing the circular conformation. The interaction between the oligosaccharide at the G6d site and protein occurs at one end of the oligosaccharide circle, in particular, at subsites +11, +12, and +13 (Figure 2). The Ile186 backbone amide hydrogen bonds to the +11 sugar 6-hydroxyl (2.61 Å). The Lys199 side chain makes hydrogen bonds with the 2- and 3-hydroxyl groups (with distances of 2.94 and 3.19 Å, respectively) of the +12 sugar. On the other face of the +12 sugar, Gly227 and Gly230 both make hydrogen bonds with the 6-hydroxyl group (2.70 and 2.94 Å, respectively). At subsite +13, double-handle hydrogen bonds once more occur, this time between the 2- and 3-hydroxyls of the sugar and the Glu190 carboxyl group (2.88 and 2.86 Å, respectively). In addition, the +13 sugar 3-hydroxyl group makes a hydrogen bond to the Asn192 backbone amide (2.75 Å).

Among the 16 sugar moieties bound in the E377A−ADP−G6 complex (three in the G6a site, two in the G6b site, five in the G6c site, and six in the G6d site), 12 of the glucose hydroxymethyl groups adopt the gauche−gauche (*gg*) conformation while three adopt a gauche−trans (*gt*) conformation. The 6-hydroxyl of the +2 sugar is in close contact with the Thr16 hydroxyl side chain, and the O5−C5−C6−O6 and C4−C5−C6−O6 torsion angles are 129.13° and −106.44°, respectively, moderately beyond the definition of a gauche conformation (30−90° or −30° to −90°). The prevalent low-energy *gt* and *gg* conformations of the hydroxymethyl group are largely reinforced by their interaction with the intraring O5 atom (2.98 Å) (Figure 2).

DISCUSSION

Overall Structural Comparison. The E377A GS−ADP−G6 complex crystal was obtained by cocrystallization of E377A GS with ADPGlc and G6 followed by soaking for 48 h in 100 mM G5. The two-domain enzyme GS displays a closed conformation when bound to HEPPSO, ADP, and glucose, which is partly due to the presence of HEPPSO in the interdomain cleft (*6*). Cocrystallization and further soaking with oligosaccharides bring four oligosaccharides to GS E377A, one bound in the interdomain cleft overlapping the HEPPSO binding site and three bound on the surface of the N-terminal domain. However, the closed conformation is maintained, and in fact, the crystal form and cell dimensions are identical to those of the E377A GS−HEPPSO−ADP structure previously determined (*6*) (Table 1). The rmsd between the Cα atoms of the E377A−ADP−HEPPSO complex and the E377A−ADP−G6 complex is only 0.34 Å (*23*). Therefore, neither the crystal packing nor the protein structural organization of GS was affected by replacement of HEPPSO inside the interdomain channel with oligosaccharide or by oligosaccharide binding on the enzyme surface. The

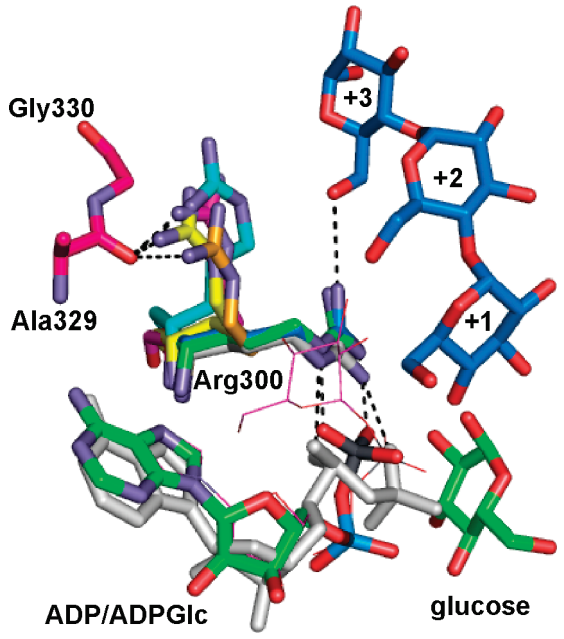

FIGURE 4: Arg300 side chain that flips out of the GS active site and stays close to Ala329 and Gly330 (shown as sticks with carbons colored hot pink) in the structures of the apo *E. coli* GS double mutant (dmGS, C7S/C408S, R300 carbon in yellow), *E. coli* GS E377A complexed with ADPGlc (*6*) (R300 carbon in magenta), apo-AtGS [PDB entry 1rzv, R299 (equivalent to *E. coli* GS R300) carbon in orange], and apo PaGS [PDB entry 2bis, R257 (equivalent to *E. coli* GS R300) carbon in cyan]. The Arg300 side chain is close to the ADP moiety in ligand-bound GS structures, such as ADP, Glc-bound wtGS (PDB entry 2qzs, R300 carbon in green), oligosaccharide-bound E377A (R300 carbon in blue), and ADP-bound AtGS [PDB entry 1rzu, R299 (equivalent to *E. coli* GS R300) carbon in white]. The ADP molecule in the AtGS complex is uniformly colored white. The carbon atoms of ADP and the glucose molecule in the wt GS complex are colored green. The ADP in the oligosaccharide-bound E377A structure occupies a superimposable position relative to the wt GS complex and is not shown for the sake of clarity. Maltotriose bound in the E377A complex is shown as sticks, and its carbon atoms are colored blue. ADPGlc in the E377A complex is shown as lines and colored magenta. Hydrogen bonds between the side chain of Arg300 and its equivalent residue in AtGS and PaGS are shown as dotted lines. Residues are labeled according to the *E. coli* GS sequence.

few observed side-chain conformational changes upon oligosaccharide binding occur on His139, whose imidazole ring moves 1.03 Å to form a hydrogen bond to the +2 sugar, and Ile186, which rotates its side chain to avoid being too close to the +11 sugar's 4-hydroxyl group (otherwise, the distance would be ~1.8 Å).

Arg300 Conformational Change upon Ligand Binding. The ADP−glucose−HEPPSO wt GS structure reveals that Arg300 tightly interacts with the ADP phosphate group in the active site, acting to stabilize developing negative charge on the ADPGlc phosphate to facilitate its departure from the glucose moiety (Figure 4) (*6*). Mutating Arg300 to Ala decreases enzyme activity 2600-fold (*24*). The oligosaccharide-bound GS reported here demonstrates a conformation of Arg300 virtually identical to that in the ADP, glucose-bound wt GS structure. The Arg300 side-chain NE and NH2 atoms are in the proximity of the ADP phosphate O2B (2.82 Å) and O1B (2.92 Å) atoms, and a long hydrogen bond (3.32 Å) is formed between the +3 sugar 6-hydroxyl and the Arg300 NH1 group (Figure 4). The involvement of Arg300 with the ADP moiety in the GS active site was also reported for ADP-bound AtGS, though it was not identical due to displacement of the phosphate (*4*). In contrast, when there is no ligand in the active site as in apo-dmGS, apo-AtGS, and apo-PaGS structures, the Arg300 (Arg299 in AtGS and Arg257 in PaGS) side chain flips out of the active site toward the loop of residues 327−331 where it is stabilized by a hydrogen bond from the Ala329 backbone amide and several van der Waals interactions with Ala329 and Gly330. It appears that the Arg300 side chain switches in and out of the GS active site in response to the binding of ligand ADP. However, the E377A EcGS complex structure obtained by soaking with ADPGlc is an exception because Arg300 remains close to the loop of residues 327−331 even though the ADP moiety is present in this structure. The distance between the Arg300 NH2 group and the phosphate O1B atom is approximately 10.4 Å. For a possible explanation for this result, recall that Glu377 forms hydrogen bonds from its carboxyl side chain to the glucose 2-hydroxyl in wt GS complexed with ADP and glucose. The E377A mutant lacks such a hydrogen bond, causing the glucose moiety to become disordered in the active site, possibly displacing Arg300. As a result, the Arg300 side chain may move out of the active site to avoid colliding with the now mobile glucose moiety of ADPGlc. Consistent with this idea, we do see some density for glucose in this space, though the density is too weak to build in the glucose moiety with confidence. To summarize, our structural results indicate that Arg300 plays the important catalytic role of stabilizing negative charge on the leaving group ADP. In the absence of the ADP moiety, Arg300 adopts a conformation outside the active site awaiting the binding of substrate.

Subsite 1. Superimposition of the G5-bound MalP structure (PDB entry 1L6I) and the E377A−ADP−G6 complex structure reveals that the +1 sugar in the E377A−ADP−G6 complex occupies an almost identical position to the second glucose +997 of maltopentaose in the G5-bound MalP, and the rest of the glucose units follow a similar path (*12*, *25*) (Figure 5). The edge glucose +998 in the G5-bound MalP complex overlaid well with the glucose molecule in the ADP−glucose−wt GS complex (PDB entry 2QZS) and presumably reflects the conformation of transferred glucose (−1 sugar) in GS (Figure 5). In both G5-bound MalP (*12*) and oligosaccharide-bound GS, the glucose at the MalP +998 sugar position (−1 sugar in GS) is involved in a number of hydrogen bonds from the protein which probably provides incentive for the abrupt kink between the +998 and +997 sugar and the 174.73° glycosidic angle that deviates significantly from the average value of 110° for a regular polysaccharide (Table 2) (*15*). In short, it appears that MalP and GS share an oligosaccharide binding site beyond the two critical sugar moieties involved in the transfer reaction.

Binding Site Analysis. Three sugar units are visible along the interdomain cleft in the electron density map, which means that at least two sugar units are missing as GS was cocrystallized with G6 and soaked with G5. They are likely to be disordered, as there are few opportunities to make strong interactions with the protein on the surface. Actually, the reducing sugar in subsite +3 is in the α configuration and not the β configuration, which is the more favored configuration for a terminal glucose residue. We suggest that this hydroxyl group is not the reducing end of the oligosaccharide chain and that there are at least two more α-1,4 glycosidic linkages that are invisible due to disorder.

The glucose units of the oligosaccharides in the GS E377A complex adopt the typical $^4C_1$ chair conformation (*26*). The surface-bound oligosaccharides in the G6b and G6c sites display a pseudohelical structure with preferred α-1,4 linkages, in

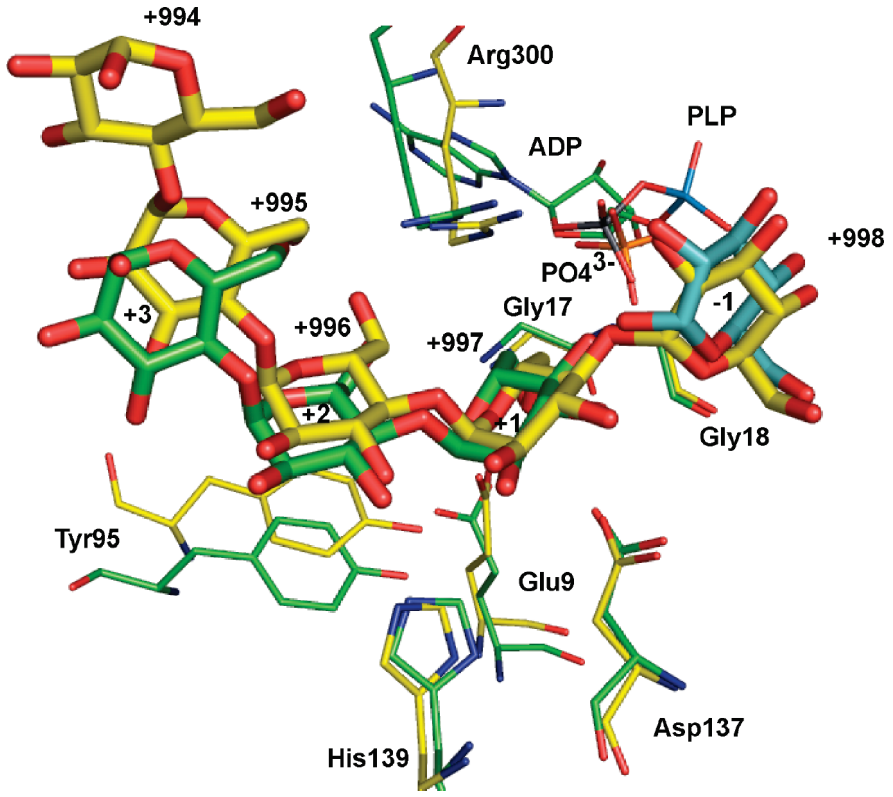

FIGURE 5: Superposition of the active site-bound oligosaccharide in the GS E377A−G6 complex (sticks, carbon in green, oxygen in red) and MalP−G5 (PDB entry 1L6I) complex (sticks, carbon in yellow, oxygen in red). The glucose (sticks, carbon in blue, oxygen in red) at subsite −1 in the ADP, Glc-bound wt GS structure (PDB entry 2QZS) is included. The GS residues interacting with oligosaccharide are shown as green lines, while the comparable residues in MalP are shown as yellow lines. ADP in E377A complex is also shown as lines (carbon in green, oxygen in blue, nitrogen in blue, phosphorus in marine). The phosphate in the active site of the MalP complex is also colored by atom (phosphorus in gray, oxygen in red). HEPPSO, which occupies a position comparable to that of oligosaccharide in the interdomain cleft in ADP, Glc-bound wt GS structure, was omitted for the sake of clarity.

agreement with the glycogen-chain model proposed by Sundaralingam (*27*) and Goldsmith et al. (*11*). The helical conformation of the glycogen main chain was termed a minimum-energy conformation that has a characteristic intramolecular hydrogen bond between the 2-hydroxyl from one glucopyranose ring and the 3-hydroxyl of the adjacent glucopyranose (*11*, *27*) . Such $O3_n-O2_{n-1}$ hydrogen bonds are retained between most glucosyl units of G6b and G6c (Table 2). In contrast, being held in the narrow interdomain cleft and possessing a relatively rich interaction with the protein, G6a was forced into an extended conformation that lacks $O3_n-O2_{n-1}$ hydrogen bonds.

The oligosaccharide at the G6a site in the GS interdomain cleft is in a most intimate association with the active site, and most interacting residues are highly conserved throughout the GS, SS, MalP, and GP families. Mutating them, for example, Asp137, Glu9, His139, or Tyr95, decreased GS specific activity to a varying extent (*15*; A. Yep and J. Preiss, unpublished results). A close inspection of the overlaid G5−MalP complex (PDB entry 1L6I) (*25*) and the E377A−ADP−G6 structure revealed that those conserved residues line the interdomain cleft and interact with the oligosaccharide in a virtually identical manner (Figure 5). This suggests that the glucan chain-binding channel is constructed in a very similar way in these enzymes to guide substrate into or acceptor out of the deeply buried catalytic site in MalP and GS, and this conclusion may apply to other GT-B fold-retaining polysaccharide processing enzymes. It is noteworthy that mutating the conserved residues described above along the interdomain catalytic channel increases the K_M of shorter oligosaccharides for EcGS but barely alters the glycogen affinity (*24*). Mutant E9A, for example, displays a 135-fold decrease in specific activity but shows no changes in affinity for glycogen or ADPGlc compared to those of wt GS. When it was assayed with maltotriose as a substrate, the affinity for the oligosaccharide decreased 7-fold and the V_{max} exhibited a 1580-fold decrease (A. Yep and J. Preiss, unpublished results). Our structure provides a possible explanation for these observations. Glycogen is a very long, branched glucan chain, certainly long enough that a single molecule of glycogen will likely span all four of the glycan binding sites identified in our structure, though they are 22−29 Å from the active site glycan binding site. The binding of glycogen would therefore not be exclusively dependent on the glycan binding site adjacent to the active site and will therefore be less sensitive to mutations of this binding site. However, a short-chain glycan is too short to reach either of the other two sites, and its binding affinity is therefore dependent exclusively on binding at or near the active site, where the mutated residues mentioned above reside. Consistent with this hypothesis is the fact that the activity of wt GS with glycogen as substrate is at least 10-fold higher [per milligram of glycan substrate; for example, 24.5 nmol of glucose transferred in 15 min at 25 mM (29 mg/mL) maltoheptaose vs 25.1 nmol for glycogen at 2.5 mg/mL] (*28*). Further, it has been observed that while glucose is not a substrate of the enzyme, maltose, maltotriose, and maltotetraose are all substrates and are progressively better with longer chain lengths (2, 13.5, and 21.9 nmol of glucose transferred in 15 min for 25 mM maltose, maltotriose, and maltotetraose, respectively).

Table 2: Conformations of Oligosaccharides Bound to GS and MalP

	ϕ^a (deg)	ψ^b (deg)	τ^c (deg)	$O2_n-O3_{n+1}$ (Å)
G6a				
(+1G)−(+2G)	99.48	120.22	114.33	3.05
(+2G)−(+3G)	66.15	85.06	106.00	3.76
G6b				
(+4G)−(+5G)	95.10	115.07	108.66	3.14
G6c				
(+6G)−(+7G)	101.96	100.76	113.00	2.85
(+7G)−(+8G)	102.50	125.86	114.16	2.92
(+8G)−(+9G)	107.60	124.62	111.48	2.83
(+9G)−(+10G)	101.58	114.42	109.21	2.96
G6d				
(+11G)−(+12G)	86.32	−51.41	114.64	5.53
(+12G)−(+13G)	101.52	119.05	115.51	3.18
(+13G)−(+14G)	120.20	123.68	116.15	2.78
(+14G)−(+15G)	114.47	128.36	114.49	2.84
(+15G)−(+16G)	47.01	104.43	110.60	4.95
maltopentaose bound to MalP (PDB entry 1L6l)				
998−997 [equivalent to (−1G)−(+1G)]	71.96	59	−174.73	4.59
997−996 [equivalent to (+1G)−(+2G)]	102.93	109.82	112.92	2.66
996−995 [equivalent to (+2G)−(+3G)]	81.19	100.03	110.99	3.48

[a] O5(n)−C1(n)−O4(n+1)−C4(n+1). [b] C1(n)−O4(n+1)−C4(n+1)−C3(n+1). [c] Glycosidic linkage angle: C1(n)−O4(n+1)−C4(n+1).

On the other hand, maltodextrins longer than four units cause little improvement in the rate (25 mM maltoheptaose gives 24.5 nmol of glucose transferred in 15 min). These results are consistent with our structure which shows that the first three glucose units tightly interact with EcGS in the active site, while the glucose units beyond three are disordered and do not apparently make strong interactions with the enzyme (*28*).

In contrast to the interdomain catalytic cleft, none of the residues at the G6c binding site are conserved in SS. However, five of seven residues interacting with surface-bound G6d use their backbone amide group. The Lys199 that forms a salt bridge to the +12 sugar is conserved in granule-bound starch synthase (GBSS) (Figure 3).

We compared several SS sequences with GS and found that there is a considerable insertion in GBSSI (K_{219}YFSGPYGE) and SSII (C_{427}YGDG) (Figure 3; only the *Arabidopsis* SS sequences are shown in Figure 3, but insertions of varying length are seen in all the SS sequences we examined) in the loop of residues 123−129 which is in the proximity of the bound maltopentaose at the G6c binding site (Figure 1). An insertion similar in length was also found at the G6d binding site in the loop of residues 190−199 in GBSSI (Y_{284}EKPQK) and SSII (P_{500}VGG) (Figures 1 and 3). These elongated loops are likely to affect glucan-chain binding at these sites.

A significant twist was found at one end between the +11 and +12 sugar moieties in G6d, probably preventing clashes with helix α8 (residues 229−237). The entire +11 sugar deviates 121.8° from the helical track suggested by the rest of G6d as the C1 (+11)−O4 (+12)−C4 (+12)−C3 (+12) angle becomes −51.41°, considerably different from the average value for a regular helix (110 ± 10°) (Table 2), but still in the allowed region. The +11 sugar forms a hydrogen bond to the +16 sugar 1-hydroxyl group, the +12 sugar 3-hydroxyl, and the Ile186 backbone amide. Overall, the oligosaccharide at G6d is more like a β-cyclodextrin with one missing glucose unit than a standard glycogen helix. This finding suggests that when glycogen binds to GS, a moderate alteration in helical conformation is possible as the local enzyme surface dictates.

Binding Mode Analysis. Distinct bidentate hydrogen bonds from a protein carboxyl side chain to the adjacent sugar 2-hydroxyl and 3-hydroxyl groups are observed at most binding sites (Asp137 at the G6a site, Asp125 at the G6c site, and Glu190 at the G6d site) and attracted our attention. Such a "bidentate" interaction was also seen in the polar interaction between the Lys199 side-chain NA atom and the +12 sugar. Removing the Asp137 carboxyl group from the interdomain catalytic cleft causes an 8140-fold decrease in GS enzyme activity (*24*). Since the +1 sugar is the immediate acceptor from the glucose of the substrate ADPGlc, its orientation is presumably critical to transfer efficiency and the bidentate hydrogen bonds from Asp137 probably play an important role in correctly positioning the +1 sugar (Figure 5). In contrast, the carbohydrate−aromatic interaction usually seen with sugar-processing proteins such as starch phorphorylase (*29*), endoglucanase CelA(*30*), and maltodextrin translocation protein maltoporin(*14*) is rare in our oligosaccharide-bound GS complex (only between Tyr95 and the +2 sugar). It appears that GS predominantly relies on hydrogen bonding and van der Waals contacts, particularly in the double-handle manner, to recognize and orient glycogen.

According to the mechanism proposed from our open apo-dmGS and closed ADP, glucose-bound wild-type GS structures, a large interdomain opening is required in each catalytic cycle as domain−domain closure forms the competent active site in the center and domain−domain opening leads to product release. On the basis of the fact that all three surface-bound oligosaccharides at the G6b, G6c, and G6d sites are located on the N-terminal domain of GS, one can conclude that glycogen binds to one domain, which means that domain−domain movement is free of constraints that could result from a two-domain spanning polyglucan. GS and SS share 32−40% sequence identity and are expected to share the same GT-B fold (Figure 3). The characteristic of a GT-B fold enzyme is that its last ~20 C-terminal residues form a helix that crosses over from the C-terminal domain to join the N-terminal domain. Sequence alignment among *E. coli* GS and SS isoforms (GBSS, SSI, SSII, and SSIII) shows that there are ~70 and ~25 residues at the beginning of the GBSS N-terminus and the C-terminus, respectively (Figure 3; note that the alignment starts at amino acid 84 for GBSS and residue 301 for SSII). Given the location of the N-terminus in the structure, the two extensions in GBSS could potentially cluster together and form an extra domain on the N-terminal domain side of the protein. The N-terminal truncation of maize SSI considerably decreases the affinity of the enzyme for amylopectin, indicating that the SS N-terminal extension modulates binding to long-chain polymers (*31*). This would therefore still be consistent with our conclusion from the oligosaccharide-bound GS structure that the N-terminal domain is responsible for glucan-chain binding, leaving the C-terminal domain free to open and close throughout the catalytic cycle.

Mechanistic Considerations. Our oligosaccharide-bound ECGS structure is consistent with the mechanism proposed for both GS and other GT-B family retaining glycosyl transferases (see Figure 4 of ref *6*) (*2*, *12*). In this mechanism, the highly conserved residues Arg300 and Lys305 serve to stabilize the developing negative charge on the leaving group ADP phosphate. As in the MalP oligosaccharide-bound structure, the only

other structure from this family that shows binding of the acceptor glycan in the active site, there is a direct hydrogen bonding interaction between the 4-hydroxyl group of the acceptor sugar and the leaving group phosphate, strongly indicating direct communication between the nucleophile and leaving group in the catalysis. This is consistent with an Sni-like mechanism, where interaction with the nucleophile is required for the labilization of the leaving group. A possibility here is that the 4-hydroxyl of the acceptor glycan actually donates the proton to the ADP leaving group, resulting in a significantly more active, deprotonated alcohol nucleophile as well. The lack of any binding in the −1 glucose donor binding site in the E377A mutant GS structure presented here is further proof of the importance of Glu377 in positioning the donor glucose moiety. Except for the loss of Glu377, the donor glucose binding site is unchanged in this structure, indicating that no significant change to this site occurs upon binding glycan. However, the absence of donor glucose occupancy in this structure means that no further light is shed regarding the issue of whether a double-displacement mechanism occurs or whether a transient oxo-carbenium cation is stabilized in the active site.

ACKNOWLEDGMENT

We thank Dr. Zdzislaw Wawrzak at DND-CAT for help with data collection and processing.

SUPPORTING INFORMATION AVAILABLE

$F_o - F_c$ electron density maps around the four bound maltooligosaccharides (Figure S1). This material is available free of charge via the Internet at http://pubs.acs.org.

REFERENCES

1. Ball, S. G., and Morell, M. K. (2003) From Bacterial Glycogen to Starch: Understanding the Biogenesis of the Plant Starch Granule. *Annu. Rev. Plant Biol. 54*, 207–233.
2. Breton, C., Najdrova, L., Jeanneau, C., Koa, J., and Imberty, A. (2006) Structures and mechanisms of glycosyltransferases. *Glycobiology 16*, 29–37.
3. Coutinho, P. M., Deleury, E., Davies, G. J., and Henrissat, B. (2003) An evolving hierarchical family classification for glycosyltransferases. *J. Mol. Biol. 328*, 307–317.
4. Buschiazzo, A., Ugalde, J. E., Guerin, M. E., Shepard, W., Ugalde, R. A., and Alzari, P. M. (2004) Crystal structure of glycogen synthase: Homologous enzymes catalyze glycogen synthesis and degradation. *EMBO J. 23*, 3196–3205.
5. Cristina, H., Guinovart, J. J., Fita, I., and Ferrer, J. C. (2006) Crystal structure of an archaeal glycogen synthase: Insights into oligomerization and substrate binding of eukaryotic glycogen synthases. *J. Biol. Chem. 281*, 2923–2931.
6. Sheng, F., Jia, X. F., Yep, A., Preiss, J., and Geiger, J. H. (2009) The Crystal Structures of the Open and Catalytically Competent Closed Conformation of *Escherichia coli* Glycogen Synthase. *J. Biol. Chem. 284*, 17796–17807.
7. Sygusch, J., Madsen, N. B., Kasvinsky, P. J., and Fletterick, R. J. (1977) Location of Pyridoxal-phosphate in Glycogen Phosphorylase-A. *Proc. Natl. Acad. Sci. U.S.A. 74*, 4757–4761.
8. Fletterick, R. J., Sygusch, J., Semple, H., and Madsen, N. B. (1976) Structure of Glycogen Phosphorylase-A at 3.0-Å Resolution and Its Ligand-Binding Sites at 6-A. *J. Biol. Chem. 251*, 6142–6146.
9. Pinotsis, N., Leonidas, D. D., Chrysina, E. D., Oikonomakos, N. G., and Mavridis, I. M. (2003) The binding of β- and γ-cyclodextrins to glycogen phosphorylase b: Kinetic and crystallographic studies. *Protein Sci. 12*, 1914–1924.
10. Bullivant, H. M., Geddes, R., and Wills, P. R. (1983) The fine structure of glycogen. *Biochem. Int. 6*, 497–506.
11. Goldsmith, E., Sprang, S., and Fletterick, R. (1982) Structure of maltoheptaose by difference Fourier methods and a model for glycogen. *J. Mol. Biol. 156*, 411–427.
12. Geremia, S., Campagnolo, M., Schinzel, R., and Johnson, L. N. (2002) Enzymatic Catalysis in Crystals of *Escherichia coli* Maltodextrin Phosphorylase. *J. Mol. Biol. 322*, 413–423.
13. Geremia, S., and Campagnolo, M. (2005) X-ray studies on protein complexes: Enzymatic catalysis in crystals of *E. coli* Maltodextrin Phosphorylase (MalP), Protein Data Bank entry 2asv.
14. Dutzler, R., Wang, Y.-P., Rizkallah, P. J., Rosenbusch, J. P., and Schirmer, T. (1996) Crystal structures of various maltooligosaccharides bound to maltoporin reveal a specific sugar translocation pathway. *Structure 4*, 127–134.
15. Yep, A., Ballicora, M. A., Sivak, M. N., and Preiss, J. (2004) Identification and Characterization of a Critical Region in the Glycogen Synthase from *Escherichia coli*. *J. Biol. Chem. 279*, 8359–8367.
16. Howard, A. J. (2000) Data processing in macromolecular crystallography. Crystallographic Computing 7: Proceedings from the Macromolecular Crystallographic Computing School (Bourne, P. E., and Watenpaugh, K. D., Eds.) Oxford University Press, Oxford, U.K.
17. Collaborative Computational Project, No. 4 (1994) The CCP4 Suite: Programs for Protein Crystallography. *Acta Crystallogr. D50*, 760–763.
18. Jones, T. A. (1978) A graphics model building and refinement system for macromolecules. *J. Appl. Crystallogr. 11*, 268–272.
19. Brünger, A. T. (1992) Free R value: A novel statistical quantity for assessing the accuracy of crystal structures. *Nature 355*, 472–475.
20. Kumar, A., Larsen, C. E., and Preiss, J. (1986) Biosynthesis of bacterial glycogen. Primary structure of *Escherichia coli* ADP-glucose:α-1,4-glucan, 4-glucosyltransferase as deduced from the nucleotide sequence of the glgA gene. *J. Biol. Chem. 261*, 16256–16259.
21. Gaspin, C., Cavaille, J., Erauso, G., and Bachellerie, J. P. (2000) Archaeal homologs of eukaryotic methylation guide small nucleolar RNAs: Lessons from the *Pyrococcus* genomes. *J. Mol. Biol. 297*, 895–906.
22. Wood, D. W., Setubal, J. C., Kaul, R., Monks, D. E., Kitajima, J. P., Okura, V. K., Zhou, Y., Chen, L., Wood, G. E., Almeida, N. F., Woo, L., Chen, Y. C., Paulsen, I. T., Eisen, J. A., Karp, P. D., Bovee, D., Chapman, P., Clendenning, J., Deatherage, G., Gillet, W., Grant, C., Kutyavin, T., Levy, R., Li, M. J., McClelland, E., Palmieri, A., Raymond, C., Rouse, G., Saenphimmachak, C., Wu, Z. N., Romero, P., Gordon, D., Zhang, S. P., Yoo, H. Y., Tao, Y. M., Biddle, P., Jung, M., Krespan, W., Perry, M., Gordon-Kamm, B., Liao, L., Kim, S., Hendrick, C., Zhao, Z. Y., Dolan, M., Chumley, F., Tingey, S. V., Tomb, J. F., Gordon, M. P., Olson, M. V., and Nester, E. W. (2001) The genome of the natural genetic engineer *Agrobacterium tumefaciens* C58. *Science 294*, 2317–2323.
23. Claude, J.-B., Suhre, K., Notredame, C., Claverie, J.-M., and Abergel, C. (2004) CaspR: A web-server for automated molecular replacement using homology modelling. *Nucleic Acids Res. 32*, W606–W609.
24. Yep, A., Ballicora, M. A., and Preiss, J. (2004) The active site of the *Escherichia coli* glycogen synthase is similar to the active site of retaining GT-B glycosyltransferases. *Biochem. Biophys. Res. Commun. 316*, 960–966.
25. Watson, K. A., McCleverty, C., Geremia, S., Cottaz, S., Driguez, H., and Johnson, L. N. (1999) Phosphorylase recognition and phosphorolysis of its oligosaccharide substrate: Answer to a long outstanding question. *EMBO J. 18*, 4619–4632.
26. Appell, M. S., Willett, J. L., and Momany, F. A. (2004) B3LYP/6-311++G** study of α- and β-D-glucopyranose and 1,5-anhydro-D-glucitol: $^4C_1$ and $^1C_4$ chairs, (3,O)B and B(3,O) boats, and skew-boat conformations. *Carbohydr. Res. 339*, 537–551.
27. Sundaralingam, M. (1968) Some aspects of stereochemistry and hydrogen bonding of carbohydrates related to polysaccharide conformations. *Biopolymers 6*, 189–213.
28. Fox, J., Kawaguchi, K., Greenberg, E., and Preiss, J. (1976) Biosynthesis of Bacterial Glycogen. Purification and Properties of the *Escherichia coli* B ADPglucose:1,4-α-D-glucan 4-α-Glucosyltransferase. *Biochemistry 15*, 849–847.
29. Schwarz, A., Pierfederici, F. M., and Nidetzky, B. (2005) Catalytic mechanism of α-retaining glucosyl transfer by *Corynebacterium callunae* starch phosphorylase: The role of histidine-334 examined through kinetic characterization of site-directed mutants. *Biochem. J. 387*, 437–445.
30. Alzari, P., Souchon, H., and Dominguez, D. (1996) The crystal structure of endoglucanase CelA, a family 8 glycosyl hydrolase from *Clostridium thermocellum*. *Structure 4*, 265–275.
31. Imparl-Radosevich, J. M., Li, P., Zhang, L., McKean, A. L., Keeling, P. L., and Guan, H. P. (1998) Purification and characterization of maize starch synthase I and its truncated forms. *Arch. Biochem. Biophys. 353*, 64–72.